

# Formation of cobalt phyllosilicate during solid state preparation of $\text{Co}^{2+}$ /ZSM5 catalysts from cobalt acetate

Mourad Mhamdi<sup>1</sup>, Eric Marceau<sup>2,\*</sup>, Sihem Khaddar-Zine<sup>1</sup>, Abdelhamid Ghorbel<sup>1</sup>, Michel Che<sup>2,3</sup>,  
Younes Ben Taarit<sup>4</sup>, and Françoise Villain<sup>5,6</sup>

<sup>1</sup>Laboratoire de Chimie des Matériaux et Catalyse, Université Tunis II-El Manar, 1060 Tunis, Tunisia

<sup>2</sup>Laboratoire de Réactivité de Surface (UMR 7609 CNRS), Université Pierre et Marie Curie, 4 place Jussieu, 75252 Paris Cedex 05, France

<sup>3</sup>Institut Universitaire de France

<sup>4</sup>Institut de Recherches sur la Catalyse (UPR 5401 CNRS), 2 avenue Albert Einstein, 69626 Villeurbanne Cedex, France

<sup>5</sup>Laboratoire de Chimie Inorganique et Matériaux Moléculaires (UMR 7071 CNRS), Université Pierre et Marie Curie, 4 place Jussieu, 75252 Paris Cedex 05, France

<sup>6</sup>Laboratoire pour l'Utilisation du Rayonnement Electromagnétique (LURE), Centre Universitaire Paris-Sud, BP34, 91898 Orsay Cedex, France

Received 10 July 2004; accepted 27 July 2004

When  $\text{Co}^{2+}$ /ZSM5 catalysts are prepared by solid state exchange between H-ZSM5 and cobalt acetate,  $\text{Co}^{2+}$  ions form layered cobalt phyllosilicate at the surface of the zeolite grains, bringing about a reassessment of the chemistry involved in the preparation of catalytic systems by solid state exchange.

**KEY WORDS:** catalysts preparation; ZSM5 zeolite; cobalt; phyllosilicate; solid state exchange; TPR; TEM; EXAFS; <sup>27</sup>Al MAS NMR.

## 1. Introduction

Transition metal ions can be introduced into molecular sieves by different methods, the most common ones being hydrothermal synthesis, liquid ion exchange (LE) or solid state ion exchange (SE). SE occurs by diffusion of transition metal ions in a zeolite *via* the heating of a mixture of two finely ground powders, the zeolite and a precursor salt containing the ions [1,2]. This method has several potential advantages. First, it is carried out at atmospheric pressure and avoids the handling of large volumes of solution. Second, LE leads to a waste in salt due to the fraction of the ions that has not been exchanged, whereas all the salt is retained by the zeolite in solid state syntheses, even if introduced in overstoichiometric ratios.

Nevertheless, a non negligible fraction of the ions does not enter the zeolite channels but remains on the outer surface of the grains as oxide particles [3,4]. An optimization of the solid state exchange method would thus consist in tuning the operating conditions and the nature of the salt to ensure the effective diffusion of the ions in the zeolite in the form of isolated species. Quantification of oxidic and isolated species can be made by techniques such as temperature-programmed reduction (TPR): as a general rule, ions inside the zeolite channels are reduced by hydrogen at higher temperatures than oxide particles [4,5]. An increase in hydrogen

consumption at high temperatures would be considered as the sign of a more successful exchange.

However, SE can involve more complex chemistry than the migration of the ions in zeolite channels or the formation of oxide particles, i.e., reactions between the precursor salt and the zeolite outer surface resulting in mixed species, which make the interpretation of thermogrammes more delicate than expected. This will be shown by studying the system  $\text{Co}^{2+}$ /ZSM5, used for example for hydrocarbons ammoxidation [6–8] and prepared here by SE from cobalt acetate and protonic H-ZSM5.

## 2. Experimental

### 2.1. Catalysts preparation

A catalyst (sample SEA) was prepared by SE between H-ZSM5 zeolite (Zeocat, Si/Al = 26) and cobalt acetate (A)  $[\text{Co}(\text{CH}_3\text{COO})_2] \cdot 4\text{H}_2\text{O}$  (Prolabo). The nominal atomic Co/Al ratio was chosen as 1.5, i.e., three times higher than the stoichiometry of protonic exchange by  $\text{Co}^{2+}$ . Powders were finely ground and mixed in a mortar for 15 min in ambient conditions. The resulting pink mixture was then heated in a helium flow ( $25 \text{ mL min}^{-1}$ ) up to  $500^\circ\text{C}$  (heating rate:  $2^\circ\text{C min}^{-1}$ ) and left at  $500^\circ\text{C}$  overnight (12 h). This treatment led to a blue powder. After washing twice the powder with deionized water and drying overnight at  $110^\circ\text{C}$  in a static oven, the colour changed to pale violet. A final treatment in  $\text{O}_2$  up to  $500^\circ\text{C}$  ( $25 \text{ mL min}^{-1}$ , heating rate:  $5^\circ\text{C min}^{-1}$ ) led to a pale pink catalyst after 1 h of treatment.

\*To whom correspondence should be addressed.

E-mail: marcean@ccr.jussieu.fr

A reference sample was prepared by SE using magnesium acetate  $[\text{Mg}(\text{CH}_3\text{COO})_2] \cdot 4\text{H}_2\text{O}$  (Acros) instead of cobalt acetate ( $\text{Mg}/\text{Al} = 1.5$ ), for the purpose of characterization by  $^{27}\text{Al}$  NMR after thermal treatment in helium. Another reference sample was prepared by a similar solid state reaction using cobalt acetate and an amorphous silica–alumina ( $\text{Si}/\text{Al} = 26$ ) instead of H-ZSM5, for the purpose of identification of the phases detected by TPR. The silica–alumina was prepared *via* sol–gel route following [9], by dissolution of  $\text{Al}(\text{sec-OC}_4\text{H}_9)_3$  (Acros) in  $\text{Si}(\text{OC}_2\text{H}_5)_4$  (Acros) in a molar ratio  $\text{Si}/\text{Al} = 26$ , addition of a tetrapropylammonium hydroxide (Aldrich)/propanol (Prolabo)/water mixture in molar ratios 0.09/8/8 with respect to Si, drying at  $110^\circ\text{C}$  and calcination at  $550^\circ\text{C}$ .

Two other samples were prepared with H-ZSM5 by three 24-h steps of LE at  $80^\circ\text{C}$  followed by washing, from a  $0.01\text{ mol L}^{-1}$  solution of cobalt nitrate (N)  $[\text{Co}(\text{NO}_3)_2] \cdot 6\text{H}_2\text{O}$  (Prolabo) (sample LEN) or cobalt acetate  $[\text{Co}(\text{CH}_3\text{COO})_2] \cdot 4\text{H}_2\text{O}$  (sample LEA). After drying in air at  $110^\circ\text{C}$ , samples LEN and LEA were treated in a helium flow ( $25\text{ mL min}^{-1}$ ) up to  $500^\circ\text{C}$  (heating rate:  $2^\circ\text{C min}^{-1}$ ) and kept at  $500^\circ\text{C}$  overnight (12 h) in the helium flow.

Solid solutions  $(\text{Co}, \text{Mg})\text{O}$ , where  $\text{Co}^{2+}$  is in octahedral symmetry (pink), and  $(\text{Co}, \text{Zn})\text{O}$ , where  $\text{Co}^{2+}$  is in tetrahedral symmetry (blue), were prepared according to Cimino and Pepe [10] and Pepe *et al.* [11], respectively, both with a ratio of 5 atoms of Co for 100 atoms of Mg or Zn, as reference samples for XANES. Commercial  $\text{Co}_3\text{O}_4$  (Merck) was used as a reference for TPR experiments.

## 2.2. Characterization

Chemical analyses were performed by ICP (Co, Si, Al) at the Vernaison Center of Chemical Analysis of the CNRS. X-Ray Diffraction (XRD) analyses were carried out on a Siemens D500 diffractometer, using  $\text{Cu K}\alpha$  radiation ( $1.5418\text{ \AA}$ ). TPR were performed under 5%  $\text{H}_2$  in argon ( $25\text{ cm}^3\text{ min}^{-1}$ ); the hydrogen consumption was measured using a thermal conductivity detector, from room temperature to  $1000^\circ\text{C}$  with a heating rate of  $7.5^\circ\text{C min}^{-1}$ . Transmission Electron Micrographs (TEM) were collected on a JEOL 100 CXII UHR microscope. Thermogravimetric analyses (TGA) were obtained on a Seiko DT-TGA 320 module operated by a Seiko SSC5200 disk station, with a heating rate of  $7.5^\circ\text{C min}^{-1}$  in a nitrogen atmosphere.

UV–Vis–NIR spectra were recorded in the reflectance mode (1 nm resolution) on a Cary 5 spectrometer (Varian) equipped with an integration sphere, using Teflon as a reference. XANES and EXAFS spectra were recorded in transmission at the Co K edge on the XAS 13 beamline of the DCI storage ring (LURE, Orsay, France). For XANES measurements, a double-crystal  $\text{Si}(311)$  monochromator was used and the energies were

scanned in 0.3 eV steps from 7680 to 7830 eV. For EXAFS measurements, a channel-cut  $\text{Si}(111)$  monochromator was used, and the energies were scanned in 2 eV steps from 7600 to 8600 eV. The energy was calibrated using a Co metal foil reference. After background correction, the XANES spectra were normalized in the middle of the first EXAFS oscillation. EXAFS analyses were performed in the framework of single-scattering treatments with the package of programmes “EXAFS pour le Mac” [12]. The Fourier transforms (FT) were calculated on  $w(k)k^3\chi(k)$ , where  $w(k)$  is a Kaiser–Bessel window with a smoothness parameter equal to 2.5. The  $k$  limits were 2 and  $11.7\text{ \AA}^{-1}$ . The FT are presented without phase correction in figure 3. Single-scattering fits of experimental curves were performed with the Round Midnight programme [13].

$^{27}\text{Al}$  MAS NMR spectra were carried out at 9.4 T over a Bruker Avance 400 spectrometer with a  $\pi/12$  single-pulse, on the following materials: the starting zeolite H-ZSM5, two samples freshly prepared by SE from cobalt or magnesium acetate after treatment in helium, and sample SEA after final treatment in oxygen. The Larmor frequency was 104.26 MHz and the MAS rate  $\omega_{\text{rot}} = 14\text{ kHz}$ .

For all techniques, the samples were characterized after cooling to room temperature and reexposure to air (it was not attempted to locate the exact positions of the  $\text{Co}^{2+}$  ions inside the zeolite after dehydration).

## 3. Results and discussion

### 3.1. Elemental analyses

The elemental compositions of H-ZSM5 and samples SEA, LEA and LEN are presented in table 1. As expected, the cobalt content is higher for SEA than for the samples prepared by liquid exchange: 94% of the cobalt ions present in the powders mixed for solid state exchange are ultimately retained on the zeolite, the remaining 6% being thus removed in the washing steps. On SEA, the significant increase of 11% of the  $\text{Si}/\text{Al}$  atomic ratio, compared with that of the starting zeolite, contrasts with the slight decrease observed on LE samples: a fraction of the aluminum ions has been lost during preparation of the sample by solid state

Table 1  
Elemental composition in cobalt, aluminum and silicium (expressed as  $\text{Si}/\text{Al}$  atomic ratio) of the starting zeolite and the three  $\text{Co}^{2+}$ /ZSM5 catalysts

Sample	Co (wt%)	Al (wt%)	Si/Al (atomic ratio)
H-ZSM5	–	1.6	25.6
SEA	5.0	1.3	28.5
LEA	1.4	1.6	24.1
LEN	0.5	1.6	24.3

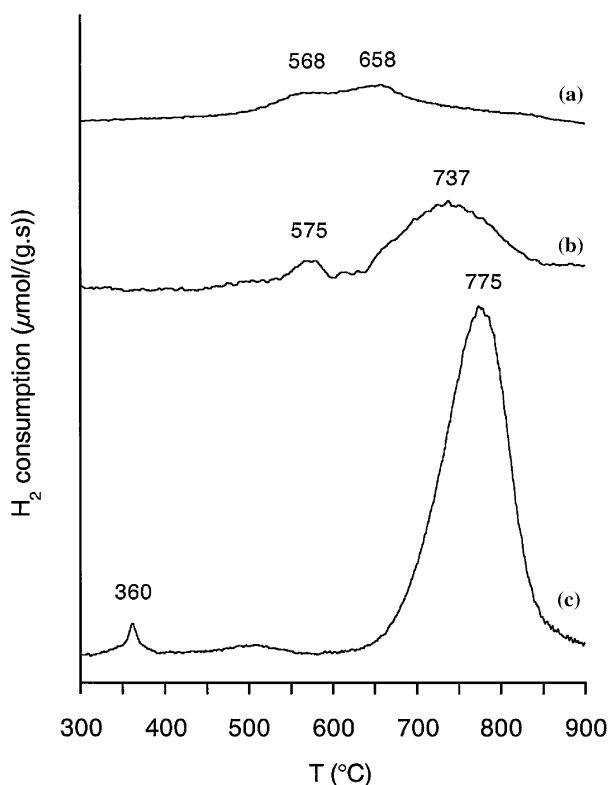


Figure 1. TPR profiles of samples (a) LEN, (b) LEA and (c) SEA.

exchange. Finally, samples prepared by liquid exchange in similar conditions but from two different salts differ by their final cobalt content. Cobalt acetate leads to a catalyst richer in cobalt than cobalt nitrate.

### 3.2. Identification of the cobalt silicate phase

X-ray diffractogrammes of the three catalysts are identical to that of the original zeolite. In the three catalysts, UV-visible spectroscopy reveals the presence of a major band at 525 nm, characteristic of  $\text{Co}^{2+}$  ions in an octahedral environment [14,15]. XANES spectra recorded at the Co K edge exhibit the same low intensity preedge (transition  $1s \rightarrow 3d$ ) as that of  $\text{Co}^{2+}$  in (Co, Mg)O, confirming the octahedral symmetry of  $\text{Co}^{2+}$  in the catalysts (maximum at 7708 eV, intensity = 0.03, compared with the intensity of the preedge for tetrahedral  $\text{Co}^{2+}$  in (Co, Zn)O = 0.08).

However the TPR thermogrammes of the three samples are different (figure 1). Broad hydrogen consumption peaks are observed for LEN between 500 and 700 °C, whereas two distinct peaks are observed for both LEA: 575 and 737 °C (broad, 93% of the total area); and SEA: 360 and 775 °C (narrow, 98% of the total area). By analogy with the reduction profile of LEN, the small peak at 575 °C is attributed for LEA to  $\text{Co}^{2+}$  ions in the zeolite; after comparison with the temperature of reduction of bulk  $\text{Co}_3\text{O}_4$  (340 °C), the small peak at 360 °C is attributed for SEA to the reduction of  $\text{Co}_3\text{O}_4$  particles. The identification of the major species reducing above 700 °C for samples SEA and LEA needs further investigation.

The sample prepared by the same solid state procedure but using an amorphous silica-alumina as support also exhibits two reduction peaks: one at 351 °C corresponding to the reduction of  $\text{Co}_3\text{O}_4$  particles, detected also by XRD and TEM, and one at 800 °C that can be attributed to a cobalt phase in “strong interaction” with the support, i.e., cobalt silicate or cobalt aluminate. On the basis of these results and the spectroscopic data presented above, the phase reducing above 700 °C on the zeolitic systems can be identified as a silicate containing  $\text{Co}^{2+}$  in an octahedral environment—an aluminate would contain  $\text{Co}^{2+}$  in a tetrahedral environment.

The TEM of samples LEA and SEA show filamentous and jagged zones surrounding or encapsulating zeolite grains (figure 2). These structures, less abundant on LEA, are observed around almost all grains on SEA and look like those attributed to phyllosilicates formed on  $\text{Ni/SiO}_2$  catalysts [16].

The identification of this phase is confirmed by X-ray absorption spectroscopy. The  $k^3$ -weighted FT obtained from the EXAFS spectrum of sample SEA is different from the one obtained for LEN. In both samples, the first coordination sphere of cobalt ions can be fitted with an octahedral environment of oxygens. But, as shown on figure 3, an intense peak due to second neighbours is seen for SEA only, indicating that  $\text{Co}^{2+}$  ions belong to a regular and crystallized structure. The first two peaks of SEA could not be fitted with parameters taken from the orthosilicate  $\text{Co}_2\text{SiO}_4$ , which would lead to a third peak between  $R = 2$  and 3 Å [17]. In contrast, a good fit was reached with structural parameters taken from talc-like

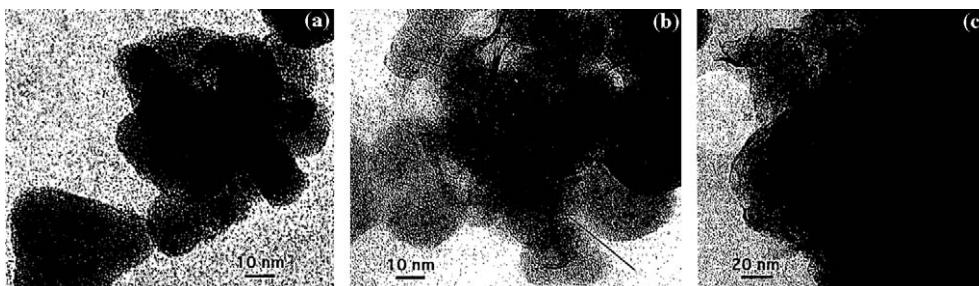


Figure 2. TEM micrographs of samples (a) LEN, (b) LEA (arrows indicate phyllosilicate layers) and (c) SEA.

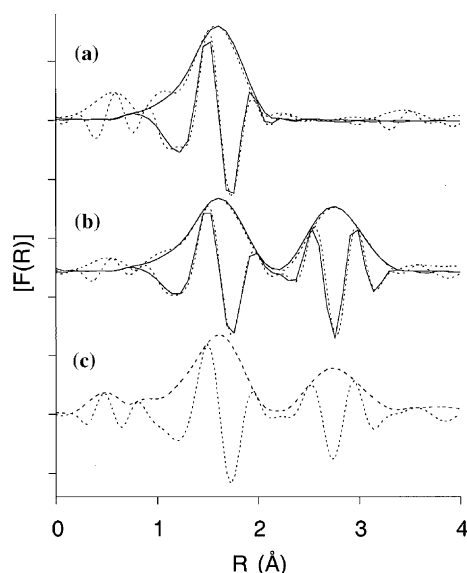


Figure 3.  $k^3$ -weighted FT of the experimental EXAFS spectra (...) recorded for samples (a) LEN, (b) SEA and (c) LEA, and the corresponding fits for the 1st and 2nd shells (—) calculated using the parameters from the table 2.

phyllosilicates (table 2) [18]. In this type of structure, in which multiple scattering has been checked to be negligible in the 0–3.5 Å distance range [18], an octahedral layer containing  $\text{Co}^{2+}$  is located between two tetrahedral layers containing silicon [19].

The FT obtained from the EXAFS spectrum recorded on LEA also exhibits a second-neighbour peak but less intense than for SEA, evidencing the lower abundance of the silicate phase in this sample. The broad TPR reduction peak at 737 °C probably encompasses the reduction of both ions inside the zeolite and phyllosilicate. Possibly due to the heterogeneity of the sample and lesser crystallinity of the silicate phase, it was not possible to obtain a satisfactory fit for the first and second shells of the FT using the parameters determined on LEN and SEA. Due to the existence of cobalt in the silicate phase outside the zeolitic framework, sample LEA contains more cobalt than sample LEN.

Table 2

Best parameters<sup>a</sup> for the fits of LEN and SEA 1st and 2nd shells

Sample	Atom	<i>N</i>	$\sigma$ (Å)	<i>R</i> (Å)	$\Delta E_0$ (eV)	$\rho$ (%)
LEN	O	6	0.08	2.07	−4	0.5
SEA	O	6	0.10	2.08	−3	0.3
	Co	6	0.10	3.13	−6	
	Si	4	0.10	3.20	−8	

<sup>a</sup>*N* = number of neighbours,  $\sigma$  (Å) = Debye-Waller factor, *R* (Å) = distance between Co and a backscatterer,  $\Delta E_0$  (eV) = energy shift,  $\rho$  (%) = agreement factor  $(\sum[k\chi_{th}(k) - k\chi_{exp}(k)]^2 / \sum[k\chi_{exp}(k)]^2)$ . <sup>b</sup>Ab initio amplitudes and phases functions for Co–O, Co–Si and Co–Co pairs were calculated using FEFF7 code [20].

### 3.3. Mechanism of formation of the phyllosilicate phase

The formation of silicates on samples LEA and SEA shows that the presence of acetate ions on the zeolite before heating is probably the key for the subsequent insertion of cobalt in a silicate matrix. In order to establish the link between the acetate ions and the mechanism of formation of the silicate,  $^{27}\text{Al}$  MAS NMR spectra were recorded on SEA systems (on the blue powder obtained after helium treatment and on the final catalyst after treatment in oxygen) and were compared with the spectrum recorded on H-ZSM5 (figure 4a, two signals at −1.2 and 52.4 ppm).

Even after 150,000 scans, the two signals observed on the blue powder obtained after helium treatment had a very low intensity (figure 4b). This is interpreted as the result of a shift of the signals out of the  $^{27}\text{Al}$  chemical shifts range usually explored (−50–100 ppm), due to perturbations caused by the proximity of paramagnetic  $\text{Co}^{2+}$  ions.

In order to reveal the changes undergone by aluminium atoms during thermal treatment under helium, a sample prepared in the same way from magnesium acetate with diamagnetic  $\text{Mg}^{2+}$  ions was studied by NMR (TGA experiments showed that dehydrated cobalt and magnesium acetates decompose in the same temperature range, 270–350 °C for cobalt acetate and 310–360 °C for magnesium acetate). As can be seen on figure 4c, heating in helium and decomposition of

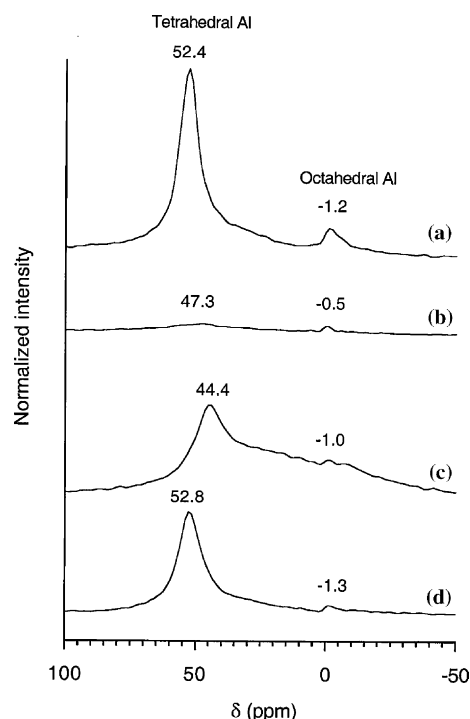


Figure 4.  $^{27}\text{Al}$  MAS NMR spectra of: (a) H-ZSM5, (b) SEA after helium treatment, (c) sample prepared from  $[\text{Mg}(\text{CH}_3\text{COO})_2] \cdot 4\text{H}_2\text{O}$  and thermally in helium and (d) SEA after  $\text{O}_2$  treatment. Spectra are presented after normalization with respect to the number of scans.

magnesium acetate resulted in the extraction of a significant fraction of aluminum ions from their tetrahedral position in the zeolite structure (new broad signal between 0 and 40 ppm).

In contrast, the spectrum recorded on catalyst SEA after the final step of preparation (figure 4d) exhibits narrow peaks corresponding to aluminum atoms in tetrahedral and octahedral positions (52.8 and  $-1.3$  ppm, respectively). Though less intense, the spectrum is quite similar to that of the initial zeolite. Taking into account the fact that UV-visible spectroscopy and XANES discard the presence of diamagnetic  $\text{Co}^{3+}$  ions, two conclusions can be drawn from this observation:

- paramagnetic  $\text{Co}^{2+}$  ions are not any more in the vicinity of the majority of the aluminum atoms in the structure; they form an extraframework phase.
- The aluminum atoms that had been extracted from the structure during heating in helium have either reintegrated the zeolitic structure, or have been eliminated during washing, as indicated by elemental analysis (section 3.1.).

The following mechanism accounting for the formation of the silicate phase in the solid state procedure can thus be proposed. The formation of the silicate is initiated during the first thermal treatment under helium, since washing removes only few  $\text{Co}^{2+}$  ions. The fragile H-ZSM5 appears to be unstable toward acetic acid produced during heating by reaction between  $\text{H}^+$  and acetates coming from the decomposition of the cobalt salt. The consequences are a superficial destruction of the zeolite grains and a local dealumination leading to a phase rich in silicon that accommodates the cobalt ions in tetrahedral symmetry (hence the blue colour of the powder) and to extraframework aluminum atoms. A parallel can be drawn with the insertion of vanadium ions inside a zeolitic framework after acidic dealumination [21]. A fraction of the aluminum atoms are eliminated during the subsequent washing. The change of colour after washing shows that the formation of the phyllosilicate as such, in which  $\text{Co}^{2+}$  ions are located in octahedral sites, starts after exposure of the silicate matrix to water and is completed during a final thermal treatment, that in  $\text{O}_2$ .

The phyllosilicate phase, though evoked by Jong and Cheng [22] also on  $\text{Co}^{2+}$ /ZSM5, is evidenced here for the first time for the preparation of a  $\text{Co}^{2+}$ /zeolite system. This reveals the limits of the detection of extraframework phases based on the interpretation of TPR results only: high quantities of cobalt can be ultimately retained on catalyst SEA, though neither in the form of isolated ions nor oxide particles. The formation of a phyllosilicate phase has been shown to occur not only during the synthesis of  $\text{Ni}/\text{SiO}_2$  catalysts, as mentioned earlier, but also during the synthesis of  $\text{Co}/\text{SiO}_2$  catalysts [23,24]. Silicate phases formation depends strongly on the preparation method; they are

generally characterized by a high temperature reduction peak in TPR, which is sometimes not entirely recorded [25–29]. However the identification of the silicate phase on  $\text{Co}/\text{SiO}_2$  catalysts is made possible by simple use of routine XRD and IR spectroscopy. This could not be done here due to the diffraction lines and IR absorption bands arising from the zeolite itself and other techniques were therefore required, like TEM and EXAFS.

In all the systems in which a silicate phase has been identified, two factors at least have usually been considered: contact of the support with water and concomitant (or subsequent) heating. However, unlike what occurs on pure silica, a preliminary step of dealumination seems to be necessary on H-ZSM5 to let the phyllosilicate form and occurs upon reaction of acetate ions with the zeolite surface during heating—which can explain why a silicate phase has not been described when the solid state exchange involves more commonly used cobalt salts such as chloride for example. The preparation of catalysts with cobalt acetate in solution shows that silicate can also be formed, but the mechanism may not be exactly the same, since no dealumination is observed.

#### 4. Conclusion

When  $\text{Co}^{2+}$ /ZSM5 catalysts are prepared from H-ZSM5 and cobalt acetate, reactions between the cobalt salt and the atoms from the zeolitic silicoaluminate framework itself can be involved, especially if the SE procedure is used, with overstoichiometric  $\text{Co}/\text{Al}$  ratios. The nature of the catalyst finally obtained depends thus strongly on the choice of the preparation method (LE or SE) and of the precursor salt (cobalt nitrate or acetate). Acetate ions attack the surface of the zeolite during heating, laying the ground for the formation of a surface cobalt phyllosilicate which could be identified only by TEM and EXAFS. Although it can be reduced at high temperature, this phase is totally different from isolated ions in exchanged positions usually associated with high temperature reduction peaks. The reaction between acetates and zeolite can lead to erroneous interpretations if the identification of the cobalt-containing phases is based only on XRD, TPR and UV-visible spectroscopy.

#### Acknowledgments

This work received the financial support of the Franco-Tunisian CMCU (action 00F1205). Dr. Xavier Carrier and Patricia Beaunier (Laboratoire de Réactivité de Surface, Université Pierre et Marie Curie) are gratefully acknowledged for their assistance in NMR measurements and in TEM, respectively. Prof. François Bozon-Verduraz (ITODYS, Université Denis Diderot) is thanked for fruitful discussion on the

preparation of reference samples for XANES and for providing access to the UV–Vis-NIR spectrometer.

## References

- [1] H.G. Karge and H.K. Beyer, *Stud. Surf. Sci. Catal.* 69 (1991) 43.
- [2] A.V. Kucherov and A.A. Slinkin, *J. Mol. Catal.* 90 (1994) 323.
- [3] R.S. da Cruz, A.J.S. Mascarenhas and H.M.C. Andrade, *Appl. Catal. B* 18 (1998) 223.
- [4] X. Wang, H.Y. Chen and W.M.H. Sachtler, *Appl. Catal. B* 26 (2000) L227.
- [5] W.M.H. Sachtler and Z. Zhang, *Adv. Catal.* 39 (1993) 129.
- [6] Y. Li and J.N. Armor, *Appl. Catal. A* 188 (1999) 211.
- [7] R. Bulánek, K. Novoveská and B. Wichterlová, *Appl. Catal. A* 235 (2002) 181.
- [8] M. Mhamdi, S. Khaddar-Zine and A. Ghorbel, *Stud. Surf. Sci. Catal.* 142A (2002) 935.
- [9] A. Carati, C. Rizzo, M. Tagliabue and C. Perego, *Stud. Surf. Sci. Catal.* 130B (2000) 1085.
- [10] A. Cimino and F. Pepe, *J. Catal.* 25 (1972) 362.
- [11] F. Pepe, M. Schiavello and G. Ferraris, *J. Solid State Chem.* 12 (1975) 63.
- [12] A. Michalowicz, EXAFS pour le Mac Logiciels pour la Chimie, Soc. Fr. Chim., Paris, (1991) 102.
- [13] F. James and M. Roos, MINUIT; CERNID Internal Report 75/20. Program Library, CERN Computing Center, CERN, Geneva, Switzerland (1976) .
- [14] Y. Okamoto, K. Nagata, T. Adachi, T. Imanaka, K. Inamura and T. Takyu, *J. Phys. Chem.* 95 (1991) 310.
- [15] A.A. Verberckmoes, B.M. Weckhuysen and R.A. Schoonheydt, *Microporous Mesoporous Mater.* 22 (1998) 165.
- [16] O. Clause, L. Bonneviot, M. Che and H. Dexpert, *J. Catal.* 130 (1991) 21.
- [17] V. Schwartz, R. Prins, X. Wang and W.M.H. Sachtler, *J. Phys. Chem. B* 106 (2002) 7210.
- [18] J.Y. Carriat, M. Che, M. Kermarec, M. Verdaguer and A. Michalowicz, *J. Am. Chem. Soc.* 120 (1998) 2059.
- [19] M. Richard-Plouet and S. Vilminot, *Solid State Sci.* 1 (1999) 381.
- [20] S.I. Zabinsky, J.J. Rehr, J.J. Ankudinov, R.C. Albers and M.J. Eller, *Phys. Rev. B* 52 (1995) 2995.
- [21] S. Dzwigaj, M.J. Peltre, P. Massiani, A. Davidson, M. Che, T. Sen and S. Sivasanker, *Chem. Commun.* (1998) 87.
- [22] S.J. Jong and S. Cheng, *Appl. Catal. A* 126 (1995) 51.
- [23] I. Puskas, T.H. Fleisch, J.B. Hall, B.L. Meyers and R.T. Roginski, *J. Catal.* 134 (1992) 615.
- [24] A. Barbier, A. Hanif, J.A. Dalmon and G.A. Martin, *Appl. Catal. A* 168 (1998) 333.
- [25] R. Trujillano, J. Grirnoult, C. Louis and J.F. Lambert, *Stud. Surf. Sci. Catal.* 130B (2000) 1055.
- [26] G.J. Haddad and J. Goodwin Jr, *J. Catal.* 157 (1995) 25.
- [27] H. Ming and B.G. Baker, *Appl. Catal. A* 123 (1995) 23.
- [28] E. van Steen, G.S. Sewell, R.A. Makhote, C. Micklethwaite, H. Manstein, M. de Lange and C.T. O'Connor, *J. Catal.* 162 (1996) 220.
- [29] C.L. Bianchi and V. Ragaini, *Catal. Lett.* 95 (2004) 61.